Journal of Magnetism and Magnetic Materials 321 (2009) 1996–2000

Contents lists available at ScienceDirect

Journal of Magnetism and Magnetic Materials

journal homepage: www.elsevier.com/locate/jmmm

Static and dynamic magnetic characteristics of $BaCo_{0.5}Mn_{0.5}Ti_{1.0}Fe_{10}O_{19}$

Saeed Choopani *, Neda Keyhan, Ali Ghasemi, Ali Sharbathi, Iman Maghsoudi, Mohammad Eghbali

Electroceramic Research Center, Department of Physics, Malek Ashtar University of Technology, Shahhin Shahr, Iran

ARTICLE INFO

Article history:
Received 28 April 2008
Received in revised form
13 December 2008
Available online 13 January 2009

Keywords:
Magnetic property
Microstructure
Susceptibility
Reflection loss

ABSTRACT

The effect of $Mn^{2+}Co^{2+}Ti^{4+}$ substitution on microwave absorption has been studied for $BaCo_{0.5}Mn_{0.5}Ti_{1.0}Fe_{10}O_{19}$ ferrite–acrylic resin composites in frequency range from 12 to 20 GHz. X-ray diffraction (XRD), scanning electron microscope (SEM), vibrating sample magnetometer, AC susceptometer and vector network analyzer were used to analyze the structural, magnetic and microwave absorption properties. The results showed that the magnetoplumbite structures for all samples have been formed. Based on microwave measurement on reflectivity, $BaCo_{0.5}Mn_{0.5}Ti_{1.0}Fe_{10}O_{19}$ may be a good candidate for electromagnetic compatibility and other practical applications at high frequency.

© 2009 Elsevier B.V. All rights reserved.

1. Introduction

The increase in electromagnetic pollution due to the rapid development of gigahertz (GHz) electronic systems and telecommunications has resulted in a growing and intense interest in electromagnetic-absorber technology. Electromagnetic interference (EMI) can cause severe interruption of electronically controlled systems. It can cause device malfunctions, generate false images, increase clutter on radar and reduce performance because of system-to-system coupling. These are some of the reasons why the use of self generated electromagnetic radiation apparatuses, which include cellular telephones, wireless computers and pagers, are strictly prohibited in certain areas; for example, in hospitals, banks, petrol stations and inside airplanes. To overcome the problems created by EMI, electromagnetic wave absorbers with the capability of absorbing unwanted electromagnetic signals, are used; and research on their electromagnetic and absorption properties is still being carried out [1,2]. Recent developments in microwave absorber technology have resulted in materials with high wave absorption coefficient, good physical performance and lower production cost [3,4]. There are a variety of absorber materials that can be used to suppress EMI depending on whether or not they are suitable for low and high frequency application [5–9]. As far as thickness and working frequency bandwidth are concerned, magnetic composites have obvious advantages. The magnetic fillers often used in such composites are ferrite materials such as spinel ferrites and hexaferrites [10,11]. Hexaferrites with planar magnetic anisotropy are greatly used as electromagnetic wave absorbers in GHz range. Barium ferrite powders are ideal fillers for the development of electromagnetic attenuation materials at microwave due to their low cost, low density, high stability, large electrical resistively and high microwave magnetic loss [12–15]. Many works have been reported on barium ferrites for use as electromagnetic materials [16–21].

In our previous paper [17–19], the microwave attenuation properties studied different doped ferrites. Here, we will report on the relationship between magnetic properties and microstructure for $BaCo_{0.5}Mn_{0.5}Ti_{1.0}Fe_{10}O_{19}$. The magnetic properties and microwave absorbing characteristics were investigated. The reason for choosing this substitute compound is their different static magnetic properties (especially, the coercivity and saturation magnetization) at the critical substitution ratio for in-plane anisotropy [20,21]. The predicated reflection loss demonstrates that $BaCo_{0.5}Mn_{0.5}Ti_{1.0}Fe_{10}O_{19}$ may be a good candidate for wave absorbing materials with low reflectivity at microwave frequency.

2. Experimental

2.1. The preparation of ferrite powders

The M-type barium ferrite with $BaCo_{0.5}Mn_{0.5}Ti_{1.0}Fe_{10}O_{19}$ composition was carried out with a conventional powder fabrication. The sample was synthesized from stoichiometric mixture of Fe_2O_3, TiO_2, Co_3O_4, $BaCO_3$ and $MnCO_3$. The mixture was crushed for 2 h and calcined in air at 1160 °C for 8 h. The heating rate of sample was from room temperature to 600 °C with 6 °C/min, and it was kept at 3 °C/min to the final sintering temperature. Calcined ferrite was crushed again for 5 h. The prepared powders are in the range 1–4 μm.

* Corresponding author. Tel.: +98 312 5227796; fax: +98 312 5225068.
E-mail address: saeedphy@yahoo.com (S. Choopani).

0304-8853/$ - see front matter © 2009 Elsevier B.V. All rights reserved.
doi:10.1016/j.jmmm.2008.12.030

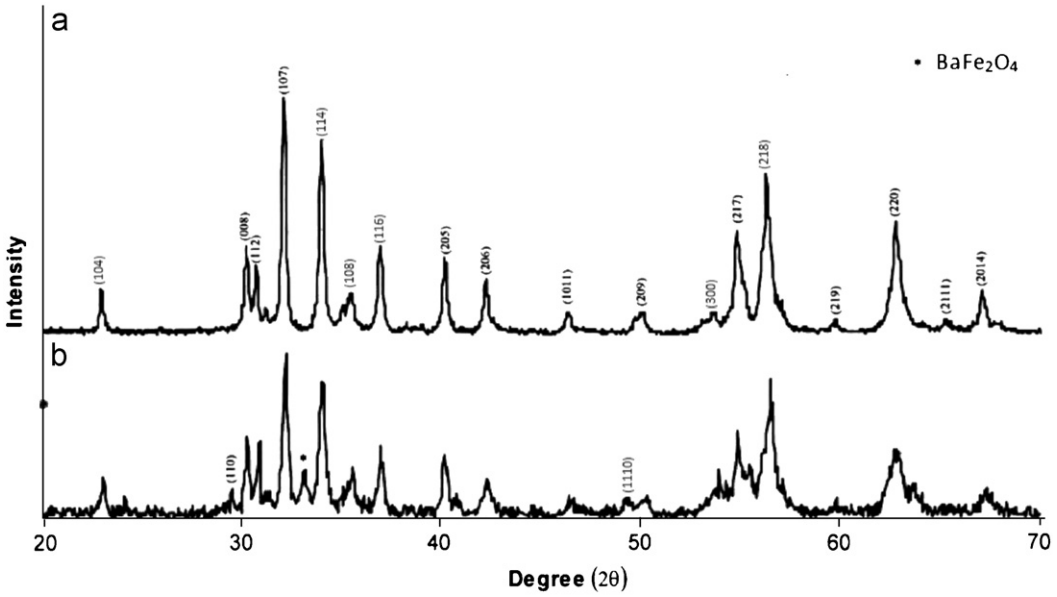


Fig. 1. XRD pattern of calcined powders at 1160 °C: (a) undoped ferrite and (b) doped ferrite.

Table 1
Lattice parameters, c/a and cell volume for doped and undoped barium ferrite.

	a (nm)	c (nm)	c/a	V (nm^3)
BaM	0.5892	2.3198	3.937	0.697
Doped BaM	0.5899	2.3233	3.938	0.700

Typical platelets have diameters to thickness ratios (D/t) ranging from 3 to 10. The composite specimens were prepared by mixing doped barium ferrite and acrylic resin powder with concentration 70:30 by weight. Mixture of ferrite powder with acrylic resin were plasticized and fired at 220 °C and 5.5 Mpa. The pressed composites were cylindrical with different thicknesses (1.35, 1.70, 1.80, 2.00, 2.10 and 2.20 mm) and a constant diameter of 40 mm.

2.2. Measurement of properties

The identification of the crystalline phase was carried out on an X-ray powder diffractometer operating at 40 kV, and by using Cu Kα radiation. Scanning electron microscopy (SEM) examinations were performed using a PHILIPS XL 400. Specimens were coated by a thin gold layer by sputtering technique for SEM observation. Vibrating sample magnetometer was used to determine the hysteresis loops of ferrite samples at room temperature. The real and imaginary parts of effective magnetic susceptibility of the sample were measured by AC susceptometer model 7000. The mass of sample was 0.25 g with a 0.001 g tolerance. Variation of the reflection loss in (dB) versus frequency in the range 12–20 GHz has been investigated.

3. Results and discussion

3.1. Microstructure characteristics

The X-ray diffraction (XRD) patterns for the calcined powder of $BaCo_{0.5}Mn_{0.5}Ti_{1.0}Fe_{10}O_{19}$ and undoped barium ferrite are shown in

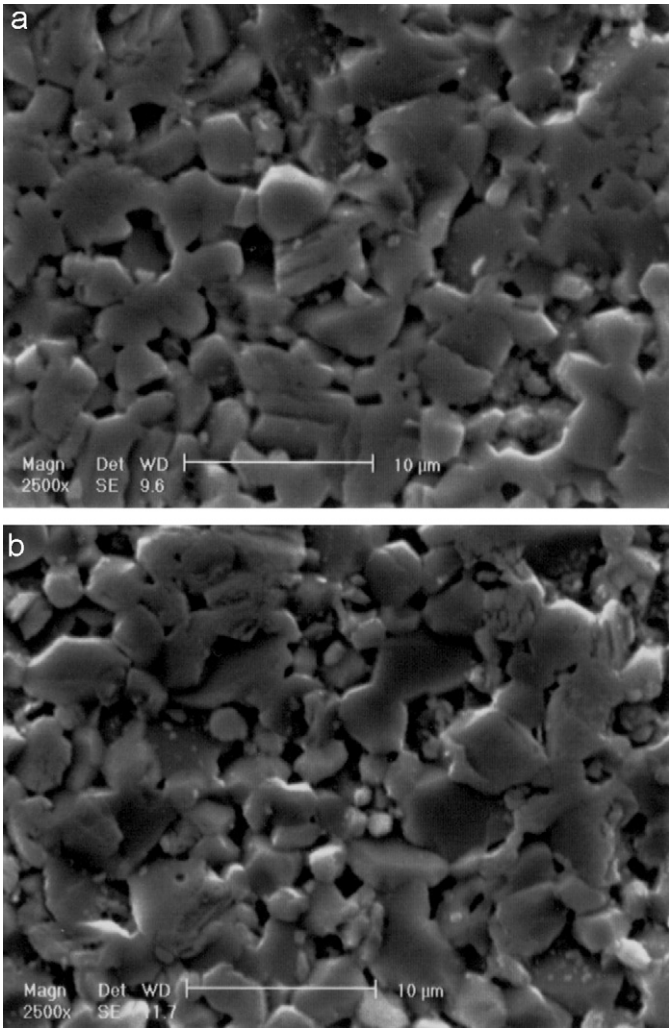


Fig. 2. SEM photographs of eroded surface of (a) undoped ferrite and (b) doped ferrite.

Fig. 1. The JCPDS file number 27-1029 was used for indexing of XRD patterns. The peaks for the doped barium ferrite appear at the same position as for the undoped ferrite, but with different intensities. Table 1 represents the related data about the lattice parameter. In the doped ferrite case, the dopants of Mn^{2+}, Co^{2+} and Ti^{4+} seem to be rearranged in the hexagonal structure to fulfill the formation of single hexagonal phase. Small amounts of anti-ferromagnetic monoferrite $BaFe_2O_4$ can be detected too. During the formation of doped barium ferrite this secondary phase has been also detected by other researchers [22]. It is generally recognized that the partial deprivation vacancy sites of Ba^{2+}, Fe^{3+} and O^{2-} can be filled with these dopant ions.

Fig. 2 shows the microstructure of eroded surface of prepared ferrite. It is found that doping with a small amount of Mn–Co–Ti does not significantly affect grain size and morphology. The grains are typical platelet morphology with grain size of about 3–6 μm. Some intergranular pores are present in the sample. Apparently, the Mn–Co–Ti doping does not contribute to the microstructure change.

3.2. Magnetic properties

The hysteresis loops of the as-synthesized barium ferrite is shown in Fig. 3. The substitution leads to decrease in H_c through the reduction of the magnetocrystalline anisotropy of the barium ferrite. It is observed that the undoped sample possess as a larger coercive force (H_c), a larger hysteresis loop area and a higher B_r than doped sample, while the former two factors may lead to a larger hysteresis loss. The H_c of pure barium ferrite is very high (about 258.7 kA/m), which is due to strong uniaxial anisotropy along the *c*-axis of M-hexaferrite. On the other hand, Mn, Co and Ti substitution lead to a rapid decrease in H_c from 258.7 kA/m (undoped) to 7.9 kA/m (doped). The moderately low H_c indicates that the domain wall motion is the dominant magnetization mechanism and the sample is a soft magnetic material.

Cho and Kim have also reported similar results for Co–Ru substituted barium ferrite [20]. However, only linear decrease in coercivity was found in Co–Ti, Co–Sn and Co–Ir substituted barium ferrite [23–25]. It is observed that coercivity is dependent upon the grain size. Based on SEM images of our doped samples described above; however, the grain sizes are not noticeably affected by the Mn–Co–Ti doping. One plausible mechanism which gives rise to the enhanced coercivity is caused by magnetocrystalline anisotropy. The easy axis of magnetization is parallel to hexagonal *c*-axis, described by anisotropy constant K_1. There is not yet a clear-cut model for the magnetocrystalline anisotropy. The contribution of dipole–dipole interaction has been

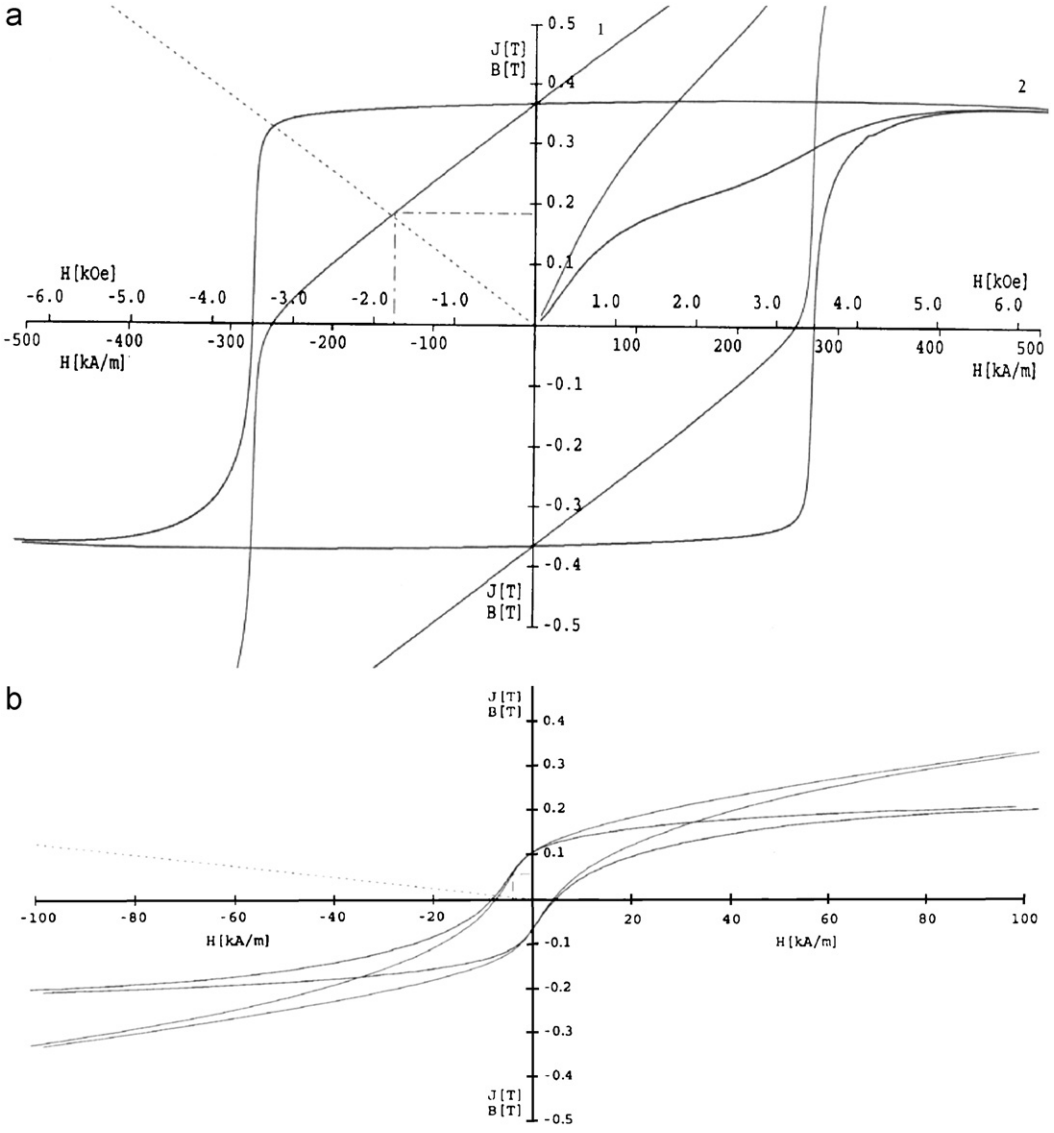


Fig. 3. Room-temperature hysteresis loops of (a) undoped ferrite and (b) doped ferrite.

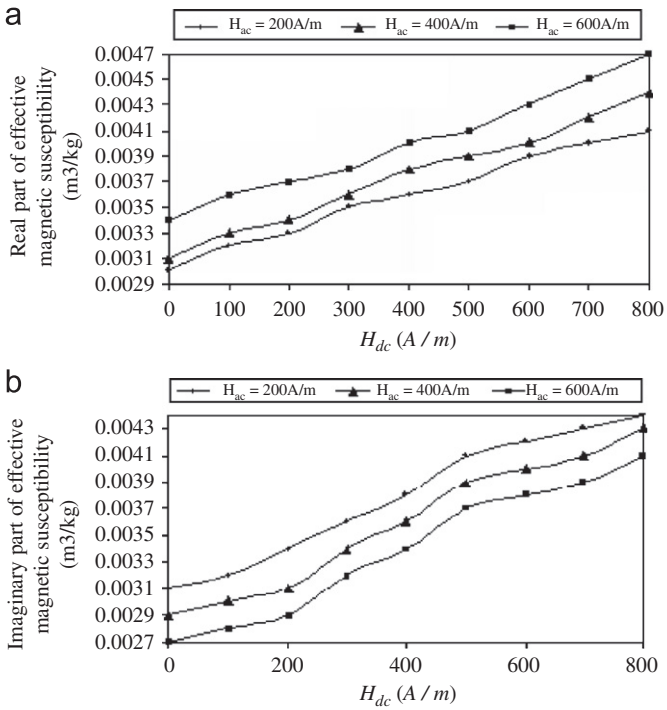


Fig. 4. Real and imaginary parts of effective magnetic susceptibility (m^3/kg) (A1) $H_{ac} = 200$ A/m, (A2) $H_{ac} = 400$ A/m and (A3) $H_{ac} = 600$ A/m.

calculated and it is relatively small. So, the spin–orbit coupling of the Fe^{3+} ions must play the main role, in spite of the fact that (free) Fe^{3+} has no orbital moment. Mostly, the contribution to the overall spin–orbit coupling is associated to the 2b site.

We assume $\mu(Fe) = 5\,\mu_B$, $\mu(Mn) = 0\,\mu_B$ and $\mu(Ti) = 0\,\mu_B$. Concerning the magnetic moment of Co^{2+} ions, we assume the $3\,\mu_B$ spin-only high-spin value when located in tetrahedral sites, and $3.7\,\mu_B$ value when located in octahedral sites. This latter is slightly higher than the spin-only high-spin value due to the partial quenching of the angular magnetic moment of these cations when located in octahedral sites.

Fig. 4 indicates the variation of real and imaginary parts of effective magnetic susceptibility with H_{DC}. The DC magnetic field was varied from 1 to 800 A/m with the period of 100 A/m. During the measurement, the test temperature was kept constant at 298 K. It is observed that effective magnetic susceptibility has linear change with increasing AC field. If there were no pinning centers in the samples, the domain walls would under the influence of external field, take an equilibrium position with minimum energy. With pinning centers, domain walls are pinned in different positions and the field exerts a pressure on them tending to shift in to an equilibrium position. The further away they are from the equilibrium position, the larger the pressure is. However pinned domain walls can still move within the potential well of pinning centers. The smaller the pressure by the field, the larger the mobility of domain walls in the potential well. When a domain wall gets released from a pinning site under the combined influence of the dc field and the ac field, it will jump to a new stable position. In the new position, it will experience a smaller pressure due to the dc field than in the old position, resulting in an increased mobility of the domain wall in the new position.

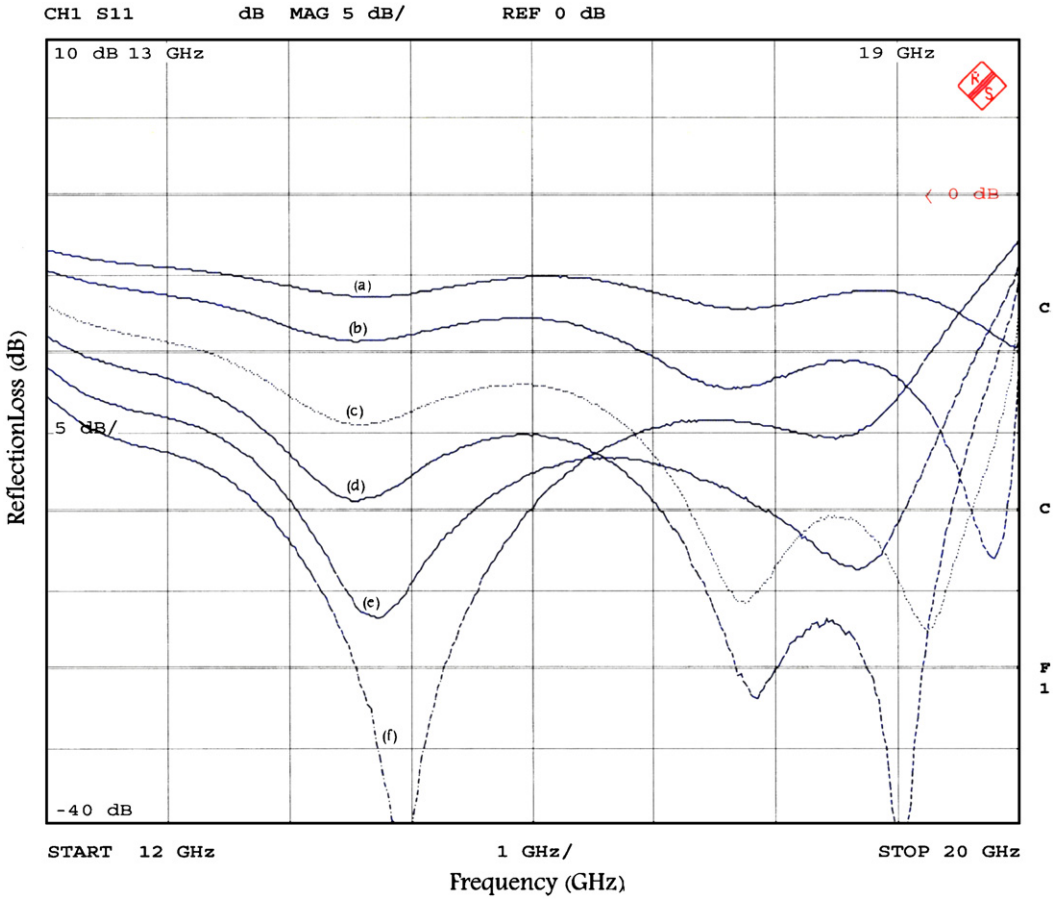


Fig. 5. Absorption characteristics of the composite: (a) $t = 1.35$ mm, (b) $t = 1.70$ mm, (c) $t = 1.80$ mm, (d) $t = 2.00$ mm, (e) $t = 2.10$ mm and (f) $t = 2.20$ mm.

Jumping back to old sites will not occur because the pressure on the domain walls, due to the dc or ac field, pushes them in one direction only. After the jump, the domain walls only oscillate in new potential wells, which is a reversible process. They do not have enough energy to jump continuously between the pinning sites.

3.3. Microwave characteristics

The reflection loss is related to the normalized input impedance Z_{in} of a metal-backed microwave absorbing layer as,

$$R(\mathrm{dB}) = 20\log\left|\frac{Z_{in}-1}{Z_{in}+1}\right| \quad (1)$$

Z_{in} is given by

$$Z_{in} = \sqrt{\frac{\mu_r^{\bullet}}{\varepsilon_r^{\bullet}}}\tanh\left[j\frac{2\pi}{c}\sqrt{\mu_r^{\bullet}\varepsilon_r^{\bullet}}fd\right] \quad (2)$$

where $\mu_r^{\bullet}$ and $\varepsilon_r^{\bullet}$ are, respectively, the complex relative permeability and permittivity of the composite medium, c is the velocity of light in free space, f is the frequency and d is the thickness of the absorber [25–30].

It is evident that the doped ferrite-containing composites have much more effective electromagnetic absorption effects. The following relation can give the ferromagnetic resonance frequency of barium ferrite:

$$2\pi f_r = \gamma\sqrt{H_\theta H_\phi} \quad (3)$$

Eq. (1) shows that the ferromagnetic resonance frequency is closely related to the magnetocrystalline anisotropy field H_θ and H_ϕ of barium ferrites. As a matter of fact, H_θ and H_ϕ are closely related to Mn^{2+}, Co^{2+} and Ti^{4+} substitutions.

Fig. 5 shows the variation of reflection loss versus frequency which was observed in composite samples with different thicknesses.

It clearly appears that the bandwidth which this ferrite can cover is about 5 GHz with average reflection loss higher than −20 dB which could be obtained at a thickness of 2.10 mm. The maximum reflection loss of this sample is −26.5 dB at matching frequency of 14.6 GHz, also there is another matching frequency at 18.6 GHz with reflection loss of −23 dB. Although these reflection loss results at matching frequency in comparison with the results of resent report Cu–Mn–Ti, Mn–Co, Ti–Co substituted barium and strontium ferrite is not considerable, but these samples are showing better wideband absorption properties [31,32]. This dispersion is due to the domain wall motion at lower frequency and spin resonance at higher frequency, respectively [33]. The matching frequency increases with a decrease in matching thickness. Such wide absorption widths and high absorption loss peaks indicate the attractive potential in microwave applications.

4. Conclusions

$BaCo_{0.5}Mn_{0.5}Ti_{1.0}Fe_{10}O_{19}$ hexaferrites are prepared by solid state reaction. Mn, Co and Ti substitutions greatly modified the magnetic properties and the microstructures of Ba-ferrites. Mn–Co–Ti mixture was very effective in reducing H_c at low level of substitution. Microwave absorbers for the applications over 12 GHz, and with satisfactory reflection losses, could be obtained at a thickness of 2.10 mm.

References

[1] S.B. Cho, D.H. Kang, J.H. Oh, J. Mater. Sci. 31 (1996) 4719.
[2] V.T. Truong, S.Z. Riddell, R.F. Muscat, J. Mater. Sci. 33 (1998) 4971.
[3] K.B. Cheng, S. Ramakrishna, K.C. Lee, Compos. Part A 31 (2000) 1039.
[4] N.C. Das, D. Khastgir, T.K. Chaki, A. Chakraborty, Compos. Part A 31 (2000) 1069.
[5] Y. Naito, K. Suetake, IEEE Trans. Microwave Theory Tech. MTT-19 (1971) 65.
[6] N. Dishovaski, A. Petkov, I. Nedkov, I. Razkazov, IEEE Trans. Magn. 30 (1994) 969.
[7] W. Grunberger, B. Springman, M. Brusberg, M. Schmit, R. Jahnke, J. Magn. Magn. Mater. 101 (1991) 173.
[8] I. Nedkov, A. Petkov, V. Karpov, IEEE Trans. Magn. 26 (1990) 1483.
[9] J.Y. Shin, T.H. Oh, IEEE Trans. Magn. 29 (1993) 3437.
[10] H.J. Kwon, J.Y. Shin, T.H. Oh, J. Appl. Phys. 75 (1994) 6109.
[11] Y. Kotsuka, H. Yamazaki, IEEE Trans. Electromagn. Comat. 42 (2000) 116.
[12] Z.W. Li, L. Chen, C.K. Ong, J. Appl. Phys. 92 (2002) 3902.
[13] O. Dubrunfaut, J. Appl. Phys. 8 (1999) 159.
[14] Y. Kim, S.S. Kim, IEEE Trans. Magn. 38 (2002) 3108.
[15] S. Sugimoto, Y. Maeda, K. Okayama, T. Maeda, H. Ota, M. Kimura, D. Book, H. Nakamura, T. Kagotani, M. Homma, Mater. Trans. JIM 40 (1999) 887.
[16] T. Nakamura, K. Hatakeyama, IEEE Trans. Magn. 36 (2000) 3415.
[17] Ali Ghasemi, Xiaoxi Liu, Akimitsu Morisako, J. Magn. Magn. Mater. 316 (2007) e105.
[18] Ali Ghasemi, Akimitsu Morisako, J. Alloys Compd. 456 (2008) 456.
[19] A. Ghasemi, A. Hossienpour, A. Morisako, X. Liu, A. Ashrafizadeh, Mater. Des. 29 (2008) 112.
[20] H. Cho, S. Kim, IEEE Trans. Magn. 35 (1999) 3151.
[21] S. Sugimoto, K. Haga, T. Kagotani, K. Inomata, J. Magn. Magn. Mater. 290–291 (2005) 1188.
[22] P. Xu, X. Han, M. Wang, J. Phys. Chem. C 111 (16) (2007) 5866.
[23] X.Z. Zhou, A.H. Morrish, Z.W. Li, Y.K. Hong, IEEE Trans. Magn. 27 (1991) 4654.
[24] X.Z. Zhou, A.H. Morrish, Z. Yang, H.X. Zeng, J. Appl. Phys. 75 (1994) 5556.
[25] J. Kreisel, H. Vincent, F. Tasset, P. Wolfers, J. Magn. Magn. Mater. 213 (2000) 262.
[26] H. Cho, S. Kim, IEEE Trans. Magn. 35 (1999) 3151.
[27] X.Z. Zhou, A.H. Morrish, Z.W. Li, Y.K. Hong, IEEE Trans. Magn. 27 (1991) 4654.
[28] X.Z. Zhou, A.H. Morrish, Z. Yang, H.X. Zeng, J. Appl. Phys. 75 (1994) 5556.
[29] W.A. Kaczmarek, B.W. Ninham, J. Appl. Phys. 76 (1994) 6065.
[30] N.H. Hur, J.Y. Park, J. Dho, S.J. Kim, E.K. Lee, IEEE Trans. Magn. 40 (2000) 2790.
[31] A. Ghasemi, A. Hossienpour, A. Morisako, A. Saatchi, M. Salehi, J. Magn. Magn. Mater. 302 (2006) 429.
[32] F. Tabatabaie, M.H. Fathi, A. Saatchi, A. Ghasemi, J. Alloys Compd., in press.
[33] B. Lax, K.J. Button, Microwave Ferrites and Ferrimagnetics, McGraw-Hill, 1962.